Lateral Cyclic Behaviour of High-Aspect-Ratio Partially Grouted Reinforced Masonry Shear Walls with Bed Joint Reinforcement

AbdelRahman AbdAllah[i], Belal AbdelRahman[ii], and Khaled Galal[iii]

ABSTRACT

Partially grouted reinforced masonry shear walls (PG-RMSWs) offer a cost-effective construction system widely used in North America. Unlike fully grouted walls, PG-RMSWs only require grouting in masonry cells that contain reinforcement, potentially reducing material and labor costs. However, limited research on the seismic performance of flexural-dominated PG-RMSWs has raised concerns about their suitability for mid- and high-rise reinforced masonry buildings. This study focuses on evaluating the lateral cyclic response of high-aspect-ratio PG-RMSWs with bed joint reinforcement (BJR) as the primary shear reinforcement. BJR not only accelerates construction but also enhances crack control. Two half-scale PG-RMSWs with an aspect ratio of 5.90 were tested under in-plane quasistatic cyclic loading, greater than the value 2.0, which is the upper limit specified for PG-RMSWs in CSA S304-14. Both walls had the same axial stress and flexural moment capacity but differed in cross-sectional design: one had a rectangular section (REC RMSW) while the other incorporated boundary elements (RMSW+BEs). The results showed that both walls exhibited flexural-dominated behavior, achieving high displacement ductility. The REC RMSW and RMSW+BEs reached ductility levels of $6.0\Delta_y$ and $12\Delta_y$, respectively, with corresponding force modification factors of 4.76 and 9.63. These findings suggest that the current design restrictions in CSA S304 should be revised to allow partial grouting in the plastic hinge region for high-aspect-ratio RMSWs, improving their applicability in seismic regions.

KEYWORDS

Partially grouted; Reinforced masonry, Boundary elements, Rectangular shear walls, Quasistatic cyclic test, Bed-joint reinforcement, Displacement Ductility.

[i] Ph.D. Candidate, Department of Building, Civil, and Environmental Engineering, Concordia University, Montreal, Quebec, Canada, H3G2W1. E-mail: abdelrahman.abdallah@concordia.ca.
[ii] Postdoctoral Fellow, Department of Building, Civil, and Environmental Engineering, Concordia University, Montreal, Quebec, Canada, H3G2W1. E-mail: belal.abdelrahman@concordia.ca.
[iii] Professor, Department of Building, Civil, and Environmental Engineering, Concordia University, Montreal, Quebec, Canada, H3G2W1. E-mail: khaled.galal@concordia.ca.

INTRODUCTION

In North America, reinforced masonry (RM) is widely recognized for its effective soundproofing and fire resistance, making it a popular construction method. To counter lateral forces from earthquakes and wind, reinforced masonry shear walls (RMSWs) are commonly used as the primary seismic force–resisting system (SFRS). These walls are classified as fully grouted (FG-RMSWs) or partially grouted (PG-RMSWs) based on grouting practices. Fully grouted walls are entirely filled with grout, while partially grouted walls have grout only in cavities containing reinforcement, resulting in lower stiffness and strength compared to FG-RMSWs.

The economic and practical benefits of PG-RMSWs have driven significant research interest, particularly in horizontal reinforcement methods such as bond beam reinforcement (BBR) and bed joint reinforcement (BJR), as depicted in Fig 1(a). BJR involves placing steel reinforcement within mortar joints, eliminating the need for grouted courses and thereby enhancing construction efficiency and cost-effectiveness relative to bond beam systems.

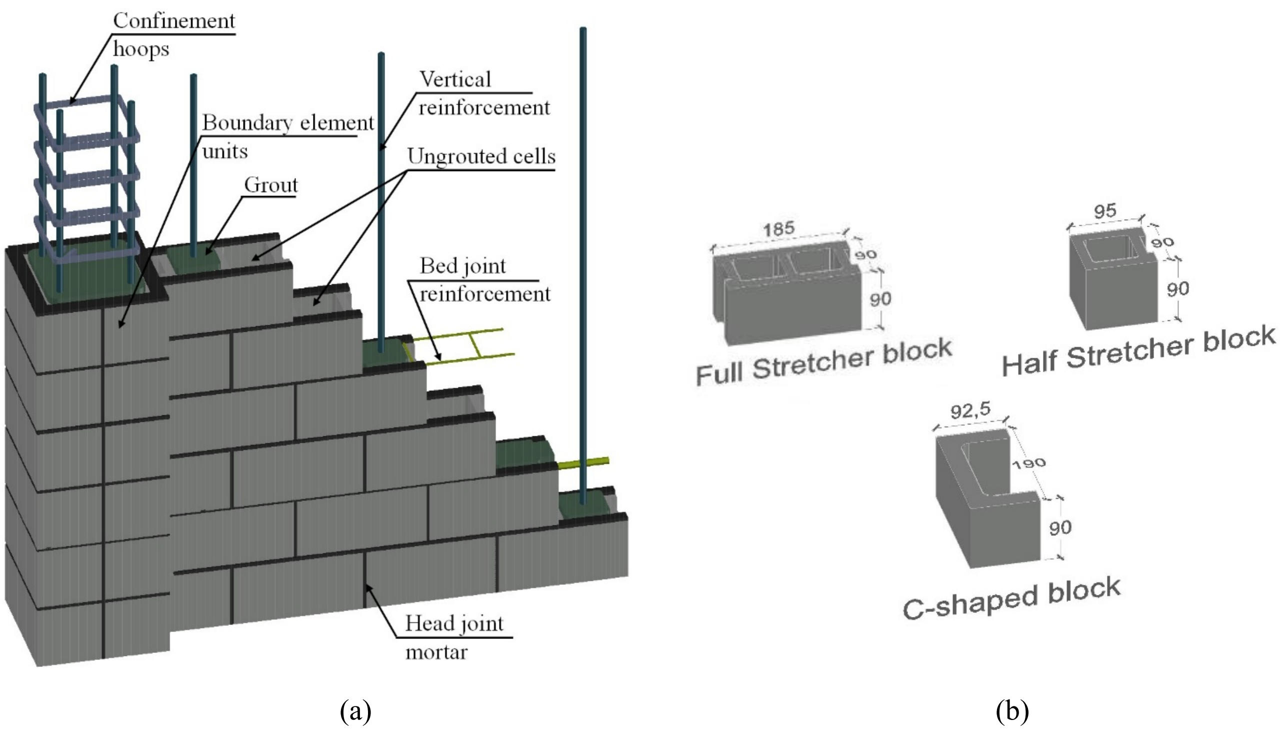

Figure 1: (a) PG-RMSWs details using BBR or BJR, and (b) Half scale block used.

Experimental studies on PG-RMSWs have primarily focused on shear-dominated walls due to CSA S304-14's [1] restrictions on their use in low-rise buildings. Schultz [2,3] examined the impact of joint reinforcement compared to bond beams in shear-dominated PG-RMSWs, finding that joint reinforcement improved lateral resistance and energy dissipation. Ramirez et al. [4] tested ladder-type reinforcements under cyclic loads, demonstrating that higher horizontal reinforcement ratios increased shear strength, particularly in slender walls. Baenziger and Porter [5] observed that joint-reinforced walls exhibited higher shear capacity and better ductility than bond beam walls. Stathis et al. [6] highlighted the superior energy dissipation and stiffness retention of joint-reinforced walls under cyclic loading. Calderón et al. [7] emphasized the complementary benefits of combining BBR and BJR systems, particularly in managing cracks and enhancing seismic performance.

For FG-RMSWs, the inclusion of boundary elements (BEs) has been shown to significantly improve performance by reducing masonry crushing, enhancing stability, and increasing ductility. Despite these advancements, there remains limited research on the flexural behavior of PG-RMSWs with high aspect ratios. Furthermore, CSA S304-14 [1] prohibits partial grouting in the plastic hinge region for such walls.

This study addresses these gaps by experimentally evaluating the cyclic behavior of flexurally dominated PG-RMSWs using bed joint reinforcement as the primary horizontal reinforcement. Two half-scale walls were tested: one with a rectangular cross-section (REC RMSW) and another with boundary elements (RMSW+BEs). The investigation focused on hysteretic response, damage progression, ductility, energy dissipation, and damping, aiming to assess the potential of PG-RMSWs with BJRs as SFRS in mid-rise RM buildings.

EXPERIMENTAL PROGRAM

Specimens' Details

At Concordia University's Structures Laboratory, two half-scale PG-RMSWs were tested under constant axial loads and in-plane quasistatic cyclic conditions. Half-scale concrete masonry blocks, as shown in Fig. 1(b), laid in a running bond pattern with 5 mm mortar joints, were used due to testing frame limitations. One wall had a rectangular cross-section, while the other included boundary elements (BEs) constructed from C-shaped concrete blocks in a stack-bond pattern to accommodate a confined steel cage for enhanced lateral performance. More details about the walls' selection and design is available at AbdAllah [8].

The walls were designed following CSA S304-14 [1] and NBCC 2020 [9] standards for moderately ductile shear walls, with a ductility-related force modification factor (R_d) of 2.0 and an overstrength-related force modification factor (R_o) of 1.5. To ensure flexural failure, the design incorporated a shear capacity exceeding the factored shear forces associated with the wall's probable moment of resistance, as specified by the capacity design approach.

Both walls shared similar axial stress levels (2.15 MPa) ($\approx 10\% f'_m$), aspect ratios (5.90), and flexural capacities. Only the 1.525 m plastic hinge region was built for testing, with higher floor effects simulated through synchronized bending moments and horizontal displacements.

The dimensions and reinforcement details for the two walls are depicted in Fig. 2. For the rectangular RMSW, 10 M rebars were used, resulting in a vertical reinforcement ratio of 0.76%. The RMSW+BEs employed #3 rebars , yielding of vertical reinforcement ratio of 0.64%. In the RMSW+BEs, D4 deformed structural wires were utilized as seismic hoops with 135° hooks, enclosing one vertical rebar in the boundary elements. These hoops were spaced 40 mm apart to meet CSA S304-14 [1] confinement and buckling prevention requirements. Horizontal reinforcement consisted of D8 wires with 180° hooks at the boundary element side and 90° hooks at the web side to improve shear flow resistance at the web-boundary interface.

Both walls were designed with equivalent flexural capacities to isolate the effect of cross-sectional configuration. Experimental results showed the flexural capacities of the REC RMSW and RMSW+BEs were 459 kN·m and 470 kN·m, respectively, reflecting only a 2.5% difference, due to material variability . However, lateral load capacities were 64.7 kN for the REC RMSW and 77.3 kN for the RMSW+BEs, marking a 19% higher capacity for the latter, attributed to variations in wall height despite identical aspect ratios. These capacities included contributions from compression reinforcing bars.

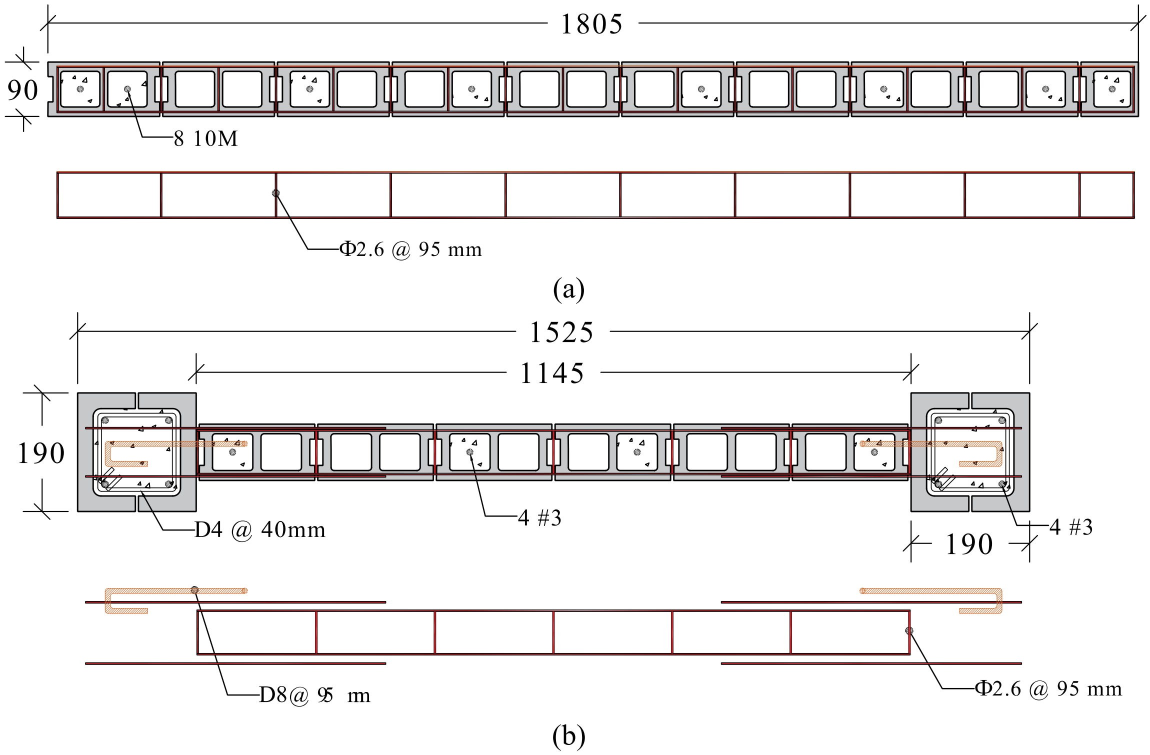

Figure 2: Dimensions and reinforcement details of the tested walls: (a) REC RMSW; and (b) RMSW+BEs. (all dimensions in mm)

Both walls incorporated ladder-shaped bed joint reinforcement (BJR) as horizontal shear reinforcement, placed at every mortar-bed joint. This setup achieved a horizontal reinforcement ratio of 0.12%, allowing vertical reinforcement to be positioned within the ladder shape. CSA S304-14 [1] specifies that BJR diameters should not exceed half the mortar joint thickness, with a maximum vertical spacing of two masonry courses between reinforcements. Each ladder unit consisted of two 2.6 mm diameter longitudinal steel wires, nearly half the 5 mm mortar joint thickness in the tested walls, connected by welded transverse ties spaced at 190 mm intervals, as depicted in Fig. 2. This wire diameter was chosen to maintain the shear resistance required for a flexural failure mode. Although the diameter slightly exceeded the 2.5 mm code limit by 0.1 mm, shear bond tests on both half- and full-scale specimens confirmed that this minor deviation did not compromise the mortar-to-block shear bond strength. Certified masons constructed the walls using Type-S normal-strength mortar, while prebagged fine grout was employed to fill the grouted cells, ensuring continuous and void-free grouting.

Materials' Properties

The wall construction utilized multiple materials, including reinforced concrete for the footing and loading beam, masonry blocks, mortar, grout, and reinforcing rebars, each serving specific structural functions. Material sampling and characterization were performed per North American standards (CSA and ASTM). Table 1 provides a summary of the material properties and their coefficients of variation (C.O.V.). For D4, D8 deformed wires, and ladder-shaped BJR, yield strengths were determined using a 0.2% strain criterion due to the absence of distinct yield points.

A triplet shear test was conducted to assess the mortar-to-block shear bond strength in the presence of the ladder-shaped bed joint reinforcement (BJR) and to examine its influence on both full-scale and half-scale masonry assemblages. A test matrix comprising 12 ungrouted assemblages was developed, divided equally between full-scale and half-scale configurations, with and without BJR. Each group included three triplet shear prisms, consisting of a single masonry unit in length and three courses in height, as illustrated in Fig. 3. This test aimed to evaluate the impact of BJR on the shear bond performance between the mortar and block.

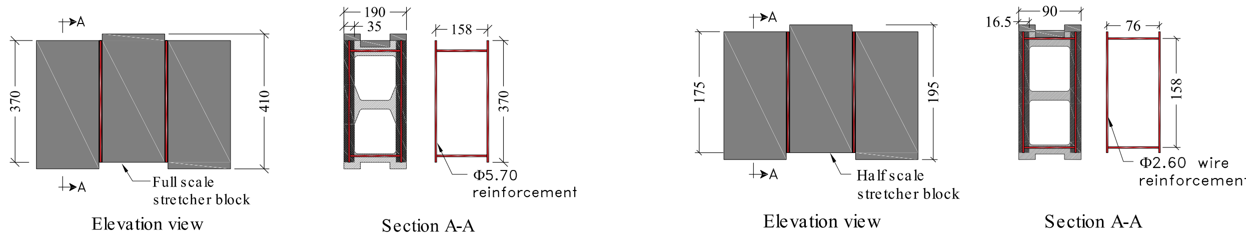

(a) (b)

Figure 3: Configurations of the shear bond assemblages (a) full scale and (b) half scale.

Four LVDTs were installed at the specimen's corners to measure average shear stress. Results from full- and half-scale assemblies, shown at Table 1, indicated that BJR did not impact shear bond strength as long as mortar contact at the block-mortar interface was maintained. Minor differences in strength were due to natural masonry variability.

Table 1: Materials' characterization summary

Material	Test	No. of specimens	Average property (MPa)	C.O.V. (%)
Full stretcher blocks	Compression strength	5	48.9	8.4
Half stretcher blocks		5	47.2	18.9
C-Shaped blocks		11	29.3	11.9
Mortar		5	21.8	17.1
Grout		5	26.8	4.7
Ungrouted prisms (4-courses)		5	22.8	6.9
Grouted prisms (4-courses)		5	20.3	14.5
BE prisms (4-courses)		5	11.2	13.6
D4 wire	Tension strength (yield/ultimate)	5	600 / 647	2.8 / 2.2
D8 wire		5	528 / 575	4.2 / 0.8
10M rebar		5	475 / 662	1.4 / 1.1
#3 rebar		5	450 / 679	5.9 / 4.8
Φ2.6mm BJR		5	480 / 697	2.8 / 5.5
Full scale-without BJR	Shear bond strength	3	0.4	13.6
Full scale-with BJR		3	0.42	16.7
Half scale-without BJR		3	0.35	13.2
Half scale-with BJR		3	0.31	14.5

Instrumentations, test setup and loading protocol

The lateral response of both walls was tracked using external and internal instrumentation. External monitoring involved 28 LVDTs and 7 potentiometers, shown at Fig. 4, to measure curvature profiles, shear deformations, potential uplift at the wall footing, sliding displacements, and strain profiles. Potentiometers recorded lateral deformations along the wall height. Internally, 5 mm strain gauges were affixed to outermost vertical rebars to assess local strains and yield locations, particularly at the footing surface and wall base. All instrumentations were linked to a digital data acquisition system with a recording rate of 10 readings per second.

(a) (b)

Figure 4: Walls' elevation view before testing: (a) REC RMSW, and (b) RMSW+BEs.

The two tested walls represented the plastic hinge region of a medium-rise reinforced masonry building. To focus on this critical area, only the first floor was constructed in the lab, while the effects of the upper floors were simulated through a loading protocol. Testing involved applying lateral displacements and a top overturning moment to replicate the influence of higher floors. The setup included three MTS hydraulic actuators: one horizontal actuator in displacement control mode for lateral displacements and two vertical actuators in force control mode to simulate axial load and overturning moment. This system, located at Concordia University's Structures Laboratory, as shown in Fig. 5 (a), utilized a rigid steel frame secured to the lab's strong floor with a reinforced concrete footing and high-strength bolts.

Horizontal displacements were applied at the wall's center of gravity. To prevent out-of-plane movements at the load application point, steel beams were connected to the rigid frame on either side, supported by thick steel plates and rods. The system allowed in-plane movements using greased polytetrafluoroethylene (PTFE) sheets on both sides of the wall, minimizing friction while permitting translational and rotational motion.

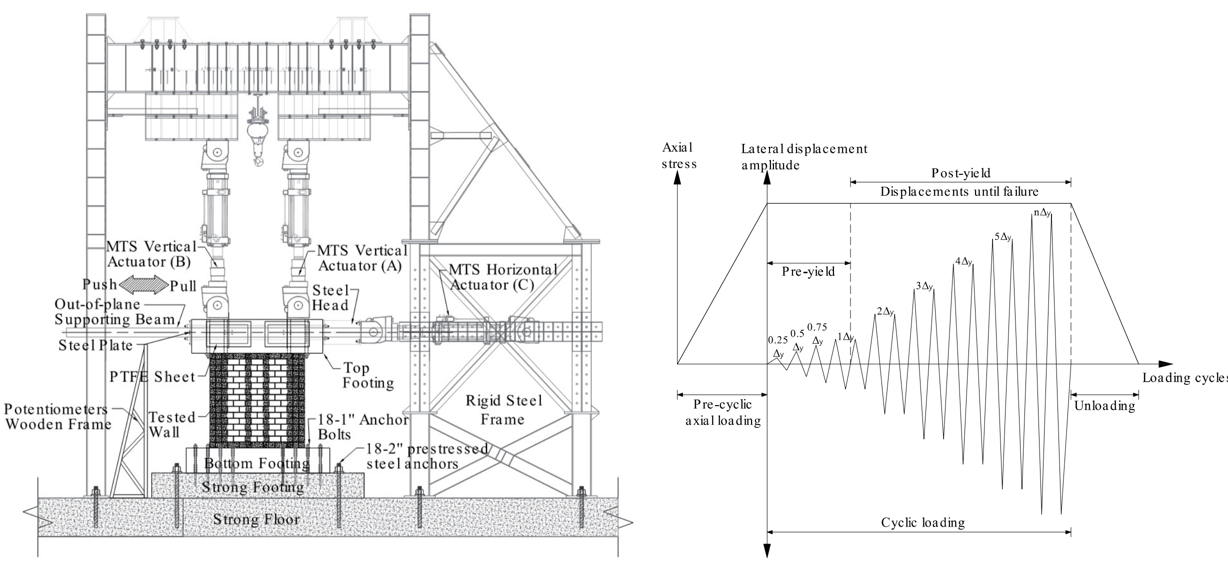

(a) (b)

Figure 5: (a) Testing setup, and (b) quasistatic cyclic loading protocol.

The two walls were subjected to a constant axial compressive stress of 2.15 MPa throughout the loading process. To replicate the overturning moment induced by lateral displacements, a coupling force (tension on one side and compression on the other) was applied, ensuring the required moment corresponded to each lateral displacement imposed by the horizontal actuator. Actuators A and B applied the axial and coupling forces, while actuator C applied the lateral displacements. The compensating moment was derived based on an inverted triangular lateral load distribution over the wall height, representing the first mode shape. The lateral displacement protocol adhered to FEMA 461 [10] and ASTM E2126 [11] standards, as shown in Fig. 5(b). The yield displacement (Δ_y), the displacement at which the outermost vertical rebars yielded, was used as the damage benchmark. This yield displacement was determined after cycling through incremental displacements at 25%, 50%, 75%, and 100% of the rebar yield strain, calculated as the average of push and pull directions. Subsequent testing involved double cycling at displacement multiples (i.e., $2\Delta_y$, $3\Delta_y$, $4\Delta_y$, $5\Delta_y$, etc.) to evaluate in-cycle strength and stiffness degradation. Testing concluded when either a 20% strength degradation or structural instability due to failure and cracking was observed, whichever occurred first.

RESULTS

Damage Progression

The two tested walls exhibited a flexure-dominated response, characterized by significant horizontal cracking and the flexural yielding of vertical reinforcement. For the REC RMSW wall, the outermost vertical rebars yielded at an average displacement (Δ_y) of 2.35 mm and a lateral force (Q_y) of 51.06 kN. Horizontal cracks initially formed at the wall toes and progressively widened as loading increased. At a displacement of $4\Delta_y$, the wall reached its maximum lateral strength (Q_u) of 68.9 kN at Δ_{Qu} of 9.66 mm, with stepped cracks appearing in the wall's mid-height. As the test continued, face shell spalling and grout splitting occurred at $5\Delta_y$, followed by masonry crushing over four courses and rebar buckling at $6\Delta_y$. This led to a 24.2% reduction in lateral load capacity, with testing ending at Δ_u equals 14.52 mm and a lateral drift ratio of 0.95%.

In contrast, the RMSW+BE wall demonstrated superior performance. The first yielding of the vertical rebar occurred at Δ_y equals 2.80 mm with Q_y of 62.08 kN, accompanied by uniform horizontal cracks along the boundary elements at $1\Delta_y$. The wall achieved its peak lateral strength (Q_u) of 79.69 kN at Δ_{Qu} equals 8.09 mm ($3\Delta_y$), with horizontal and stepped cracks extending along the wall height. Notably, the RMSW+BE wall maintained its lateral load capacity nearly unchanged up to $12\Delta_y$, showing only a 6% reduction. As loading progressed, spalling and compression toe crushing were observed in the boundary elements, along with rebar buckling at $10\Delta_y$. By $12\Delta_y$, extensive stepped and flexural cracking led to instability, ending the test at Δ_u of 33.42 mm and a drift ratio of 2.19%. It should be noted that these drift values were calculated at the top of the tested portion of the wall in the laboratory, under the assumption that the remaining untested section behaves elastically. This assumption implies that the overall drift ratio remains the same throughout the wall.

The final damage state for both tested walls is shown at Fig. 6. Overall, the RMSW+BE wall outperformed the REC RMSW wall, achieving higher lateral capacity, displacement, and drift ratios while sustaining its load capacity for a longer duration.

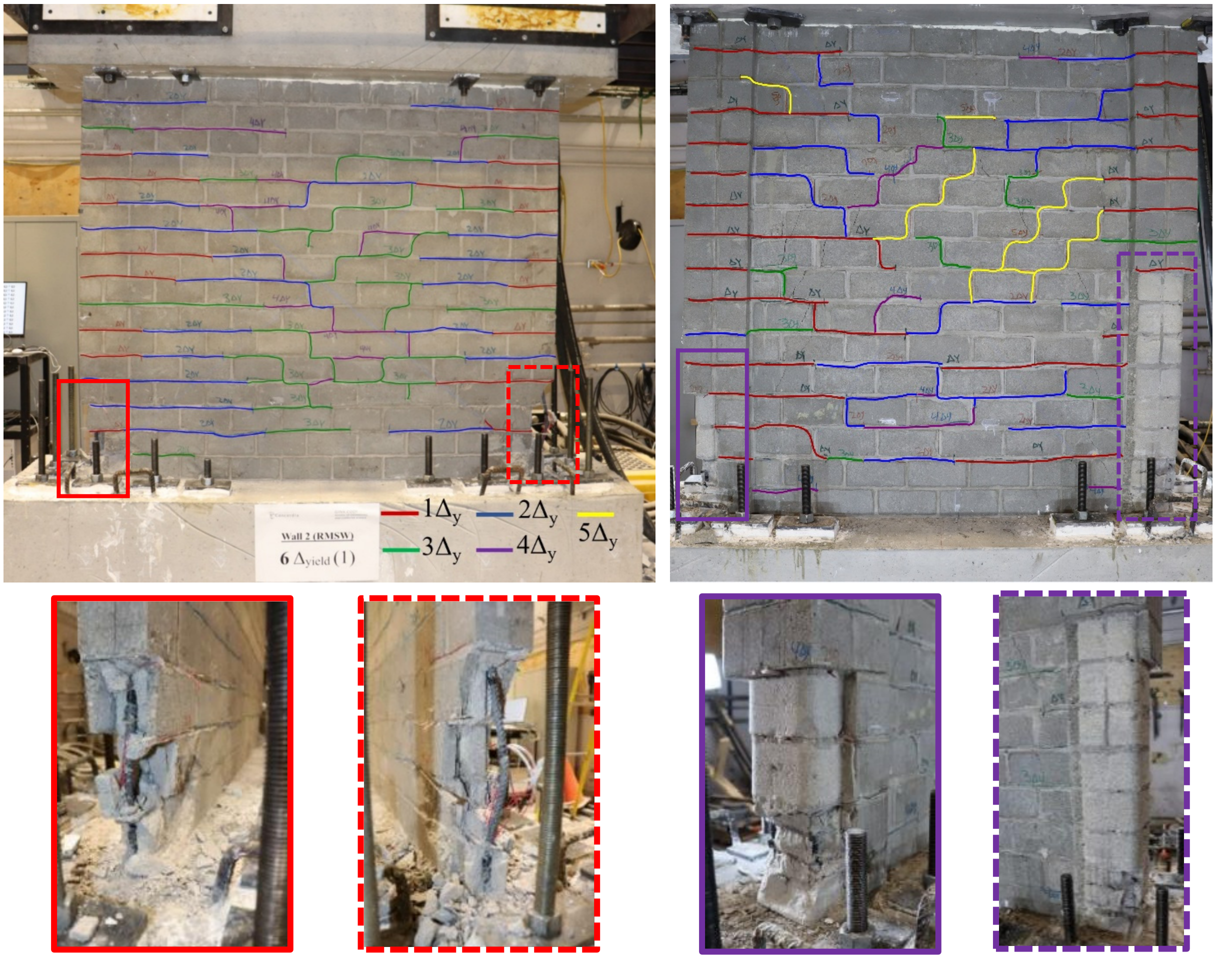

(a) (b)

Figure 6: Final damage and crack pattern for (a) REC RMSW, and (b) RMSW+BEs.

Hysteretic Response, Ductility and Response Modification Factors

The hysteresis loops for the REC RMSW and RMSW+BEs walls, shown in Fig. 7, illustrate their lateral response under cyclic loading. The horizontal axes represent lateral displacement (Δ) and drift ratio (Δ/H_{lap}), while the vertical axis indicates lateral resistance (Q). Key loading stages, including displacements, lateral loads, and curvatures, are summarized in Table 2.

Both walls displayed nearly symmetric cyclic responses in the push and pull directions, with a flexural response characterized by the yielding of the outermost vertical rebars before the appearance of diagonal or stepped shear cracks. Ductile behavior was evident in both specimens, as they endured significant inelastic deformations with minimal reduction in lateral load capacity. However, this ductility was more pronounced in the RMSW+BEs wall due to the added confined boundary elements, enhancing its overall performance.

Ductility (μ) represents a wall's capacity to endure inelastic deformations without significant strength loss. Displacement ductility (μ_{Δ}) is defined as the ratio of the ultimate inelastic displacement before failure to the yield displacement. The ductility at maximum lateral capacity (μ_{Qu}) is calculated as the ratio of the displacement at maximum capacity (Δ_{Qu}) to the yield displacement (Δ_y). Additionally, the ultimate displacement ductility ($\mu_{\Delta u}$) is determined by the ratio of ultimate displacement (Δ_u) to yield displacement.

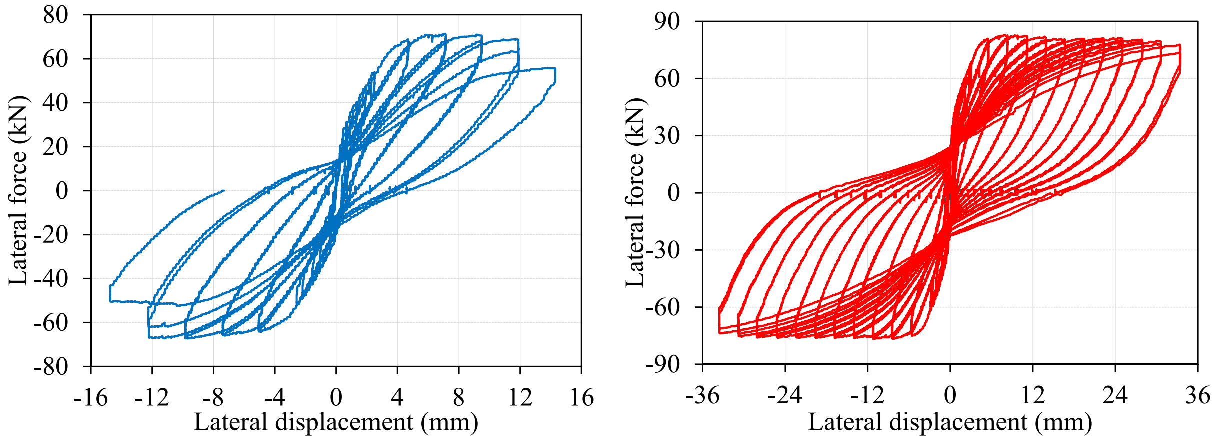

(a) (b)

Figure 7: Load–displacement hysteresis loops: (a) REC RMSW; and (b) RMSW+BEs.

The experimental load-displacement envelopes were idealized using the Tomazevic approach [12], which models the response as an equivalent elastic-perfectly plastic system, as shown in Fig. 8. This method involves calculating the idealized yield displacement the idealized displacement ductility at ultimate capacity (μ_{Qu-id}), and ultimate displacement ($\mu_{\Delta u-id}$). The idealized curve is constructed to match the energy absorption of the actual load-displacement envelope by ensuring equal areas under both curves. It is obtained by extending a line from the origin to the experimental yield point and continuing to the idealized lateral resistance.

Table 2 presents the measured and idealized displacement ductility for the tested walls. Both walls exhibited high displacement ductility, attributed to their post-peak hardening behavior under quasistatic cyclic loading. The RMSW+BEs demonstrated an ultimate displacement ductility that was 192% higher than that of the REC RMSW, highlighting the significant ductility improvement provided by the confined end zone. However, the RMSW+BEs displayed lower displacement ductility at ultimate capacity compared to the REC RMSW. This was due to the earlier achievement of maximum lateral capacity at $3\Delta_y$ for the RMSW+BEs, compared to $4\Delta_y$ for the REC RMSW.

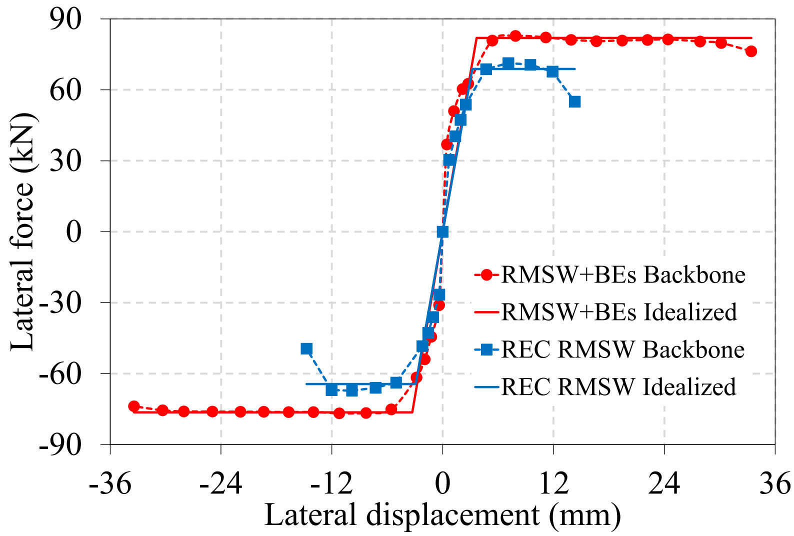

Figure 8: Experimental and bilinear idealized load–displacement envelopes for REC RMSW and RMSW+BEs.

The RMSW+BEs with BJR tested in this study achieved a notably higher ultimate displacement ductility of 11.93, compared to the 10.0 reported by AlAhdal [13] for a partially grouted wall with BBR (aspect ratio: 5.61, axial stress ratio: 8.9, vertical and horizontal reinforcement ratios: 0.64% and 0.12%, respectively). Additionally, the tested rectangular wall (REC RMSW) attained a ductility value of 6.19, which is comparable to fully grouted walls documented in the literature [14,15], despite its high aspect ratio and axial stress ratio.

According to NBCC 2020 [9], seismic response modification factors are categorized into ductility-related factors (R_d) and overstrength-related factors (R_o). Moderately ductile RMSWs are assigned an R_d value of 2.0 and an R_o value of 1.5 for moderately ductile RMSWs. The R_d value, based on idealized displacement ductility ($\mu_{\Delta u-id}$) and natural time period (T_n) according to Newmark and Hall [16], is calculated using the equal displacement approach in NBCC 2020 [9], irrespective of the structure's time period.

The overstrength factor (R_o) is defined as the ratio of wall ultimate capacity to design capacity (Q_d), with Q_d determined per CSA S304-14 [1] guidelines. Table 2 highlights response modification factors, showing that the RMSW+BEs have lower R_o values than the NBCC standard of 1.5. However, both walls demonstrated increased R_d , exceeding the NBCC standard for moderately ductile RMSWs ($R_d = 2$) and even surpassing the value for ductile RMSWs ($R_d = 3$). The RMSW+BEs exhibited an R_d value 202% higher than the REC RMSW.

The combined seismic response factor ($R = R_d \times R_o$) was 7.52 for the REC RMSW and 12.52 for the RMSW+BEs, significantly exceeding the NBCC value of 3.0 for moderately ductile RMSWs. The RMSW+BEs achieved an R-value 66.5% higher than the REC RMSW, implying that PG walls with boundary elements could be designed for 60% of the load required for PG-RMSWs with rectangular sections. This demonstrates the excellent ductility and seismic performance of PG-RMSWs with BJRs, particularly when boundary elements are incorporated, supporting their use as the main seismic force-resisting system in RM buildings.

Table 2: Summary of the measured loads, displacements, displacement ductility and seismic force modification factors of tested RMSWs

Specimen	Yield stage		Maximum capacity		Δ_u (mm)	Displacement ductility				Force modification factors	
	Q_y (kN)	Δ_y (mm)	Q_u (kN)	Δ_{Qu} (mm)		μ_{Qu}	$\mu_{\Delta u}$	μ_{Qu-id}	$\mu_{\Delta u-id}$	R_d	R_o
REC RMSW	51.1	2.4	68.9	9.7	14.5	4.12	6.19	3.17	4.76	4.76	1.58
RMSW+BEs	62.1	2.8	79.7	8.1	33.4	2.89	11.93	2.33	9.63	9.63	1.30

CONCLUSIONS

Previous studies have mainly focused on rectangular, shear-dominated PG-RMSWs, with limited research on flexurally dominated walls with boundary elements and bed joint reinforcement (BJR). This study investigates two half-scale PG-RMSWs, one with a rectangular cross-section (REC RMSW) and the other with boundary elements (RMSW+BEs), designed for flexural failure. Both walls were tested under constant axial stress and lateral cyclic loading. The results showed that both walls exhibited inelastic ductile behavior and symmetric hysteresis loops at varying displacement ductility levels. The REC RMSW showed 20% strength degradation at $6\Delta_y$, while the RMSW+BEs reached $12\Delta_y$ with a 6% reduction in lateral capacity. Failure mechanisms for both walls included face shell spalling, grout crushing, and rebar yielding/buckling, typical of flexural-dominated shear walls. The RMSW+BEs displayed a higher drift at the ultimate stage

(2.2%) compared to the REC RMSW (0.95%). The displacement ductility values were 4.76 for the REC RMSW and 9.63 for the RMSW+BEs. Seismic modification factors based on displacement ductility were 4.76 for the REC RMSW and 9.63 for the RMSW+BEs. Strength-related seismic modification factors were 1.58 for the REC RMSW and 1.30 for the RMSW+BEs, suggesting an overestimation for RMSW+BEs per the NBCC 2020. The findings support that PG-RMSWs with BJR have enhanced cyclic performance, supporting their use in medium-rise buildings in the ductile category. This highlights also the need to revisit partial grouting provisions in CSA S304, though further research is necessary to generalize these findings.

ACKNOWLEDGEMENTS

The authors would like to acknowledge the financial support of the Natural Sciences and Engineering Research Council of Canada (NSERC), Canadian Concrete Masonry Producers Association (CCMPA), Canada Masonry Design Center (CMDC), and Fonds de Recherche du Québec – Nature et Technologies (FRQNT).

REFERENCES

[1] Canadian Standards Association. CSA S304.14. Design of masonry structures. vol. 1. Ontario, Canada: 2014.

[2] Schultz AE. NIST Research Program on the Seismic Resistance of Partially-Grouted Masonry Shear Walls 1994:116.

[3] Schultz AE, Hutchinson RS. NIST GCR 01-808 Seismic Behavior of Partialy-Grouted Masonry Shear Walls, Phase 2: Effectiveness of Bed-Joint Reinforcement 2001:442.

[4] Ramírez P, Sandoval C, Almazán JL. Experimental study on in-plane cyclic response of partially grouted reinforced concrete masonry shear walls. Eng Struct 2016;126:598–617. https://doi.org/10.1016/j.engstruct.2016.08.010.

[5] Baenziger G, Porter ML. Joint Reinforcement as Primary Shear Reinforcement for Concrete Masonry Shear Walls. TMS EJournal 2018;Vol. 36, N.

[6] O. Stathis1 OF and SLL 1. Effects of horizontal reinforcement distribution on in-plane performance and post-peak behaviour of masonry shear walls. 10th Aust Mason Conf 2018:467–78.

[7] Calderón S, Sandoval C, Araya-Letelier G, Inzunza E, Milani G. Quasi-static testing of concrete masonry shear walls with different horizontal reinforcement schemes. J Build Eng 2021;38. https://doi.org/10.1016/j.jobe.2021.102201.

[8] Abdallah A, Abdelrahman B, Galal K. Lateral cyclic performance of flexural-dominated partially grouted reinforced concrete masonry shear walls with bed joint reinforcement. Eng Struct 2025;328:119587. https://doi.org/10.1016/j.engstruct.2024.119587.

[9] (NRC) NRC. National Building Code of Canada: 2020. vol. 1. 2020.

[10] Federal Emergency Management Agency (FEMA). FEMA 461-Interim testing protocols for determining the seismic performance characteristics of structural and nonstructural components. Washington D.C, United States of America: 2007.

[11] ASTM E2126-11. Standard Test Methods for Cyclic (Reversed) Load Test for Shear Resistance of Vertical Elements of the Lateral Force Resisting Systems for Buildings, West Conshohocken, PA: 2011, p. 15.

[12] Tomazevic M. Earthquake-Resistant Design of Masonry Buildings. vol. 1. Published By Imperial College Press And Distributed By World Scientific Publishing CO.; 1999. https://doi.org/10.1142/p055.

[13] Alahdal AMM. In-plane Cyclic Response of Flexural-Dominated Partially Grouted Reinforced Masonry Shear Walls with Boundary Elements. Concordia university, Montreal, Canada, 2024.

[14] Shedid MT, El-Dakhakhni WW, Drysdale RG. Behavior of fully grouted reinforced concrete masonry shear walls failing in flexure: Analysis. Eng Struct 2009;31:2032–44. https://doi.org/10.1016/j.engstruct.2009.03.006.

[15] Shedid MT, El-Dakhakhni WW, Drysdale RG. Alternative Strategies to Enhance the Seismic Performance of Reinforced Concrete-Block Shear Wall Systems. J Struct Eng 2010;136:676–89. https://doi.org/10.1061/(asce)st.1943-541x.0000164.
[16] Newmark NM., W. J. Hall. Earthquake Spectra and Design. Earthquake Engineering Research Institute Monograph Series; 1982.